https://doi.org/10.3311/PPch.43736

Periodica Polytechnica Chemical Engineering

Optimization of Hydrometallurgical Recovery of MnO_2 from Dry Cell Waste Using Response Surface Methodology

Erwan Adi Saputro[1,2,3*], Muhandis Akbar Winaji[1], Muchammad Fahrizal Hanif[1], Ardika Nurmawati[1], Ely Kurniati[1], Caecilia Pujiastuti[1]

[1] Department of Chemical Engineering, Faculty of Engineering and Science, Universitas Pembangunan Nasional Veteran Jawa Timur, Jalan Raya Rungkut Madya No. 1, 60294 Rungkut, Surabaya, Indonesia
[2] Magister of Environmental Science, Faculty of Engineering and Science, Universitas Pembangunan Nasional Veteran Jawa Timur, Jalan Raya Rungkut Madya No. 1, 60294 Rungkut, Surabaya, Indonesia
[3] Carbon Technology, Research Center, Universitas Pembangunan Nasional Veteran Jawa Timur, Jalan Raya Rungkut Madya No. 1, 60294 Rungkut, Surabaya, Indonesia
* Corresponding author, e-mail: erwanadi.tk@upnjatim.ac.id

Received: 18 February 2026, Accepted: 20 April 2026, Published online: 04 June 2026

Abstract

This study aims to recover manganese dioxide from depleted dry cell batteries using a hydrometallurgical process optimized by response surface methodology (RSM). The research is motivated by the high industrial demand for imported MnO_2 and environmental issues associated with hazardous spent battery waste. The recovery process involved microwave-assisted leaching using 1.2 M H_2SO_4 with the addition of H_2O_2 reductant (0–2% w/v), followed by oxidative precipitation using 0.25 M $KMnO_4$. Variables tested included reductant concentration and leaching time. Based on RSM optimization using the central composite design model, optimum conditions were achieved at an H_2O_2 concentration of 2% w/v and a leaching time of 39.15 min. Under these conditions, a recovery rate of 96.76% was obtained with a desirability value of 0.805 and a model R^2 of 0.9151. The final product exhibited Mn purity of 96.10–97.33%, a significant increase from the raw material (64.61%) and surpassing the commercial MnO_2 standard (>92%). This research highlights the synergistic integration of microwave-assisted heating and chemical reduction. While previous studies have applied these techniques independently, their combined effect drastically accelerates the extraction kinetics, reducing the leaching time to under 40 min, which is significantly faster than conventional methods while still achieving commercial-grade purity from complex secondary waste. This study demonstrates that microwave-assisted hydrometallurgy is a highly time-efficient and sustainable approach for recycling battery waste into high-value industrial raw materials, supporting sustainable development goals principles.

Keywords

dry cell, hydrometallurgy, leaching, manganese dioxide, RSM

1 Introduction

MnO_2 is an essential compound widely utilized across various industrial sectors. In filtration processes, MnO_2 is commonly employed as a filter medium due to its ability to adsorb iron (Fe) and manganese (Mn) ions present in wastewater [1]. In the steel industry, MnO_2 is used as a protective coating for iron-based soft magnetic composites (FeSMCs) to enhance material performance [2]. Furthermore, MnO_2 serves as an active component in lithium-ion batteries as well as zinc–manganese batteries [3]. According to data from Statistics Indonesia in 2025, Indonesia remains dependent on imports to meet domestic MnO_2 demand, with import volumes reaching 24,531,206 kg in last 2024, representing an increase of 32.32% compared to the previous year [4]. MnO_2 is classified as hazardous and toxic waste (B3) due to its potential environmental and health risks [5]. MnO_2 is an inorganic material that is soluble in acidic reagents [6, 7]. Structurally, α-MnO_2 consists of double chains of MnO_6 octahedra, whereas β-MnO_2 is composed of single-chain octahedral frameworks [8].

The maximum allowable concentration of manganese in water for hygiene and sanitation purposes, as stipulated by the Indonesian Minister of Health Regulation No. 2 year 2023, is 0.1 mg/L [9]. Exposure to MnO_2

Cite this article as: Saputro, E. A., Winaji, M. A., Hanif, M. F., Nurmawati, A., Kurniati, E., Pujiastuti, C. "Optimization of Hydrometallurgical Recovery of MnO_2 from Dry Cell Waste Using Response Surface Methodology", Periodica Polytechnica Chemical Engineering, 2026. https://doi.org/10.3311/PPch.43736

concentrations exceeding this threshold may lead to ecotoxicological effects that pose risks to human health. MnO_2 can undergo bioaccumulation through water systems, potentially causing neurological disorders and damage to internal organs [10]. In response to these challenges, the government, through the sustainable development goals (SDGs) framework, promotes the recycling of hazardous waste to mitigate environmental pollution while simultaneously fulfilling industrial demand for strategic materials, including MnO_2. A dry cell battery is a primary battery with a nominal voltage of 1.5 V, consisting of a zinc anode, a MnO_2–carbon cathode, a carbon rod, and ammonium chloride electrolyte, in which electrical energy is generated through the reduction-oxidation process. Dry cell works through a reduction–oxidation reaction, one of which is the reaction between zinc oxide and NH_4Cl that converts ZnO into zinc chloride [11–14].

MnO_2 contained in spent dry cell batteries can be separated from impurities using pyro-metallurgical, biometallurgical, and hydrometallurgical processes. Pyrometallurgy relies on high-temperature energy input, which increases operational costs and poses environmental risks due to the generation of hazardous slag and residues requiring further treatment [15]. Biometallurgy employs microorganisms to leach metals from waste materials; however, this approach demands strict control of operating conditions such as temperature, pH and nutrient availability [16]. In contrast, hydrometallurgical processing is based on the selective dissolution of metals using acidic solvents and allows the separation of soluble components from insoluble impurities. Compared to other methods, hydrometallurgy is considered to be the most efficient and practical approach for MnO_2 recovery, as it operates at relatively low temperatures and does not require microbial management. This method involves metal dissolution in strong acid solutions, followed by purification steps to obtain MnO_2 with high purity and recovery efficiency [17, 18].

Hydrometallurgical processing involves the dissolution of metals in strong acidic solutions under controlled heating, followed by purification steps to obtain high-purity metal products [18–22]. Previous studies have demonstrated that microwave-assisted heating significantly enhances metal extraction efficiency [23, 24]. Lin et al. [25] reported a MnO_2 leaching yield of 95.07% using microwave heating, which was approximately 20% higher than that achieved with conventional heating when using 1.2 M H_2SO_4 and liquid to solid ratio 10 mL/g. Similarly, Chang et al. [26] observed a MnO_2 leaching efficiency of 90% under microwave-assisted hydrometallurgical conditions from manganese ore. In addition to heating methods, the use of reducing agents can enhance metal extraction efficiency from metal ore [22, 27]. In other study, 0.8 M H_2O_2 has been shown to substantially improve MnO_2 leaching efficiency from manganese ore, reaching up to 99.04% under conventional hydrometallurgical conditions [28].

To determine optimal operating conditions, response surface methodology (RSM) is employed to evaluate the combined effects of multiple independent variables on the extraction response [29]. RSM integrates factorial techniques and ANOVA to model response variables, primarily through the application of either central composite design (CCD) or Box-Behnken design (BBD) [30–32]. Specifically, CCD utilizes five factor levels and axial points to achieve high precision in surface curvature estimation, whereas BBD operates on only three levels, offering greater experimental efficiency by excluding extreme corner points [30, 33]. While CCD is particularly suitable for sequential modeling and robust prediction, BBD provides a more cost-effective alternative when operational safety or physical constraints prevent the use of extreme parameter combinations [34–36]. In this study, hydrometallurgical processing of spent dry cell batteries is conducted using microwave-assisted heating combined with H_2O_2 as a reducing agent. Key variables, including extraction time and reductant dosage, are analyzed using a CCD to identify optimal conditions that optimize manganese leaching recovery from spent dry cell waste.

2 Experimental

2.1 Instrumentation

This study was conducted at the Biomass and Energy Laboratory, Faculty of Engineering, Universitas Pembangunan Nasional "Veteran" Jawa Timur, Surabaya, Indonesia. The experimental work and data analysis were carried out from January to June 2025. Materials used in this study include "ABC" dry cell batteries collected from household waste in the city of Surabaya, H_2SO_4 (98%), H_2O_2 (50%), $KMnO_4$ (99%), and dihydrated oxalic acid ($H_2C_2O_4 \cdot 2H_2O$, >98%) all is extra pure for analysis grade supplied by CV (Chemical Indonesia Multi Sentosa, Surabaya). Demineralized water used in this study was obtained from UD (Nirwana Abadi, Surabaya). The instrument used in this study include modified Electrolux Microwave Model EMG23K22B with magnetic stirrer and 40 cm Allihn condenser which

operates power at 240 W and 300 rpm of stirring as shown in Fig. 1. Permanganometric titration and an X-ray fluorescence (NEX QC+, Rigaku, Tokyo, Japan) equipped with QuanTEZ software and a detector of < 160 eV @Mn K-alpha line, were used to determine the MnO_2 composition on solid sample. From the permanganometric analysis (according to ASTM E465-24 [37]) the MnO_2 composition was calculated by Eq. (1).

$$\%MnO_2 = \frac{\left(\frac{m_{H_2C_2O_4}}{EW_{H_2C_2O_4}} - V_{KMnO_4} \times N_{KMnO_4}\right) \times EW_{MnO_2}}{m_{sample}} \times 100\% \quad (1)$$

The $m_{H_2C_2O_4}$ is the mass of added oxalic acid (g), $EW_{H_2C_2O_4}$ is the equivalent mass of oxalic acid (g/eq), V_{KMnO_4} is the volume of potassium permanganate titrant used (L), N_{KMnO_4} is the normality of the potassium permanganate solution (eq/L), EW_{MnO_2} is the equivalent mass of manganese dioxide (g/eq), and m_{sample} is the mass of the dry cell sample (g).

2.2 Preparation

The manganese-carbon mixture was recovered by stripping the zinc casing from spent dry cells and washing it with demineralized water until the filtrate reached a neutral pH 7 to ensure the complete removal of residual electrolytes. The resulting black residue was subsequently oven-dried at 110 °C for 1 h and pulverized to a particle size of 150 mesh (99.33 µm) to enhance the surface area for optimal extraction efficiency. The chemical composition of the prepared "ABC" dry cell sample used in this study was determined by X-ray fluorescence (XRF) and is given in Table 1.

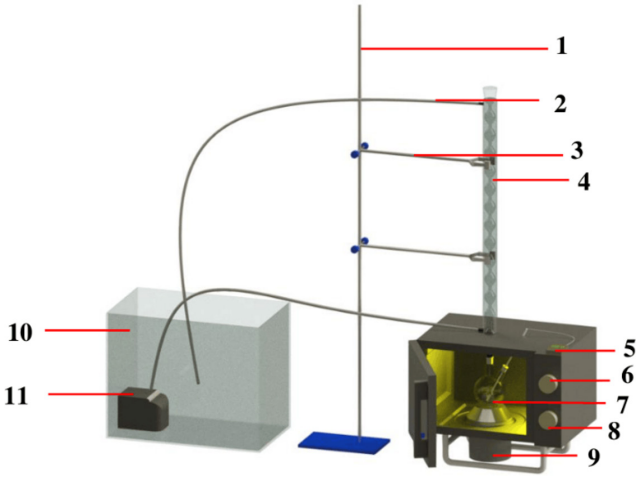

Fig. 1 Microwave-assisted instrumentation. 1. Stand, 2. Hose, 3. Clamp, 4. Condenser, 5. Thermocouple, 6. Power set, 7. 500 mL two neck flat bottom flask, 8. Time set, 9. Magnetic stirrer, 10. Water tank, 11. Water pump

Based on Table 1, the chemical composition can be calculated using Eqs. (2)–(5).

$$m_{MnO_2} = \frac{m_{Mn}}{MW_{Mn}} \times MW_{MnO_2} \quad (2)$$

$$m_{ZnCl_2} = \frac{m_{Cl}}{2 \times MW_{Cl}} \times MW_{ZnCl_2} \quad (3)$$

$$m_{ZnO} = \left(\frac{m_{Zn}}{MW_{Zn}} - \frac{m_{Cl}}{2 \times MW_{Cl}}\right) \times MW_{ZnO} \quad (4)$$

$$\%mass_i = \frac{m_i}{m_{total}} \times 100\% \quad (5)$$

The m_{Mn} is the mass of manganese (g), m_{Cl} is the mass of chlorine (g), m_{Zn} is the mass of zinc, m_{MnO_2} is the mass of MnO_2 (g), m_{ZnO} is the mass ZnO compound (g), m_{ZnCl_2} is mass of $ZnCl_2$ (g), MW_{Mn} is the molar mass of Mn, MW_{Cl} is the molar mass of Cl, MW_{Zn} is the molar mass of Zn (g/gmol), MW_{MnO_2} is the molecular mass of MnO_2, MW_{ZnO} is the molecular mass of ZnO, MW_{ZnCl_2} is the molar mass of $ZnCl_2$, $\%mass_i$ is the mass percentage of compound *i*, m_i is the mass of compound *i*, and m_{total} is the total mass of the sample. The results of the calculations by Eqs. (1)–(5) are shown in Table 2. The spent dry cell contains $ZnCl_2$ because it works through a reduction–oxidation reaction, one of which is the reaction between zinc and NH_4Cl that converts zinc to $ZnCl_2$.

2.3 Microwave-assisted leaching

10 g of the prepared sample was dissolved in 100 mL 1.2 M H_2SO_4 with a 0–2% w/v solvent of H_2O_2 and subsequently subjected to microwave-assisted leaching. The process was conducted at a power of 240 W, a stirring speed of 300 rpm, and a temperature of 80 °C for 10–50 min. Following the reaction, the mixture was filtered to isolate the carbon residue. The filtrate was collected for the subsequent precipitation stage to obtain purified MnO_2.

Table 1 XRF analysis of "ABC" dry cell sample

Composition	Mn	Zn	Cl
%mass	58.78	40.46	0.76

Table 2 Chemical composition of prepared the "ABC" dry cell sample

Composition	MnO_2	ZnO	$ZnCl_2$
%mass	64.61	34.37	1.02

2.4 Oxidative precipitation

Precipitation was carried out by adding 0.25 M $KMnO_4$ until the solution attained a persistent purple coloration, followed by a 20-min reaction period at 25 °C under constant stirring at 300 rpm. Upon filtration, the residue was washed with demineralized water until the filtrate became colorless to ensure the complete removal of excess $KMnO_4$. The resulting MnO_2 deposit was subsequently oven-dried at 110 °C for 1 h.

2.5 Optimization model

RSM was employed to model the manganese recovery from the spent dry cells through a hydrometallurgical process, specifically utilizing a CCD to evaluate the interaction and significance of H_2O_2 concentration (*A*) and leaching time (*B*). A face-centered CCD ($\alpha = \pm 1$) comprising 10 experimental runs with two center-point replicates was executed via *Design Expert* Version 13.00 [38] to identify the optimal operational conditions for maximizing the recovery percentage. The response can be represented graphically, either in the three-dimensional space or as contour plots that help visualize the shape of the response surface. The ranges and the levels of the factors investigated in the model are given in Table 3.

3 Result and discussion

3.1 Characterization

The purity of the recovered MnO_2 was analyzed using the ASTM E465-24 [37] permanganometric titration using Eq. (1), followed by X-ray Fluorescence (XRF) analysis to verify the results, with the corresponding recovery data across various H_2O_2 concentrations and leaching times presented in Table 3.

Fig. 2 shows consistently high MnO_2 purity between 95.36–97.74% in several conditions with standard error between 0.72–5.87% based on ASTM E465-24 [37] permanganometric analysis. Based on XRF analysis in Table 4, the chemical compounds composition can calculate using Eqs. (2)–(5).

Table 4 shows that the final precipitate achieved a MnO_2 purity 95.95–97.15%, a substantial increase from the 64.61% found in the raw material as shown in Table 2.

Table 3 Central composite design factors and independent variables

Variable (unit)	Factor	Levels		
		−	0	+
H_2O_2 (%w/v)	*A*	0	1	2
Time (min)	*B*	10	30	50

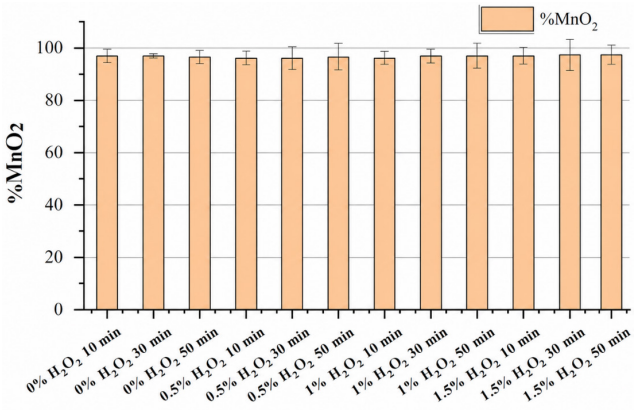

Fig. 2 Purity of MnO_2 based on ASTM E465-24 [37] permanganometric analysis

This enhancement demonstrates that the hydrometallurgical process using 1.2 M H_2SO_4, H_2O_2 as a reductant, microwave-assisted leaching and oxidative precipitation can effectively eliminated major impurities. Specifically, ZnO levels (in $ZnSO_4$ form) dropped from 34.37% to 2.50–3.66%, while $ZnCl_2$ decreased from 1.02% to 0.21–0.59%.

The process efficiency is attributed to the use of $KMnO_4$ as a precipitator, which selectively reacts with dissolved manganese to form MnO_2 deposits. In the study by Peng et al. [39], the selection of extraction parameters was carefully justified from both chemical and thermodynamic perspectives. The use of 1.2 M H_2SO_4 was chosen based on stoichiometric considerations to provide optimal H^+ activity capable of fully dissolving the zinc and manganese oxides from the complex dry cell matrix. Using a lower concentration could lead to incomplete dissolution due to acid depletion during the reaction. Conversely, utilizing a higher concentration would result in an excessive amount of unreacted free acid in the system, which not only increases the consumption of neutralizing agents in the subsequent precipitation stage but also risks equipment corrosion under microwave irradiation [39].

Furthermore, the solid-to-liquid ratio (mass of solid material to the volume of solution) was selected to ensure the optimal mass transfer and uniform heating. A highly concentrated slurry increases viscosity, leading to uneven microwave energy distribution (hotspots) and poor leaching kinetics, whereas a highly dilute solution decreases the economic viability of the process. Finally, the choice of H_2O_2 concentration within the 0–2% (w/v) range is justified by its stability under microwave heating. While H_2O_2 is an excellent reducing agent for converting insoluble Mn^{4+} to soluble Mn^{2+}, concentrations exceeding 2% under intense microwave irradiation rapidly undergo auto-decomposition into

Table 4 Chemical composition based on XRF analysis

Factor		Elements			Compounds		
H_2O_2 (%w/v)	Time (min)	Mn	Zn	Cl	MnO_2	$ZnSO_4$	$ZnCl_2$
0	10	97.67	2.02	0.32	96.95	2.66	0.39
	30	97.76	1.92	0.32	97.10	2.51	0.39
	50	97.35	2.29	0.36	96.54	3.02	0.44
0.5	10	97.01	2.67	0.32	95.95	3.66	0.39
	30	96.91	2.59	0.50	96.10	3.30	0.60
	50	97.53	2.27	0.20	96.54	3.22	0.24
1	10	97.23	2.51	0.26	96.18	3.51	0.31
	30	97.38	2.30	0.32	96.51	3.11	0.38
	50	97.76	2.03	0.21	96.91	2.84	0.25
1.5	10	97.77	1.93	0.30	97.08	2.56	0.36
	30	97.71	2.05	0.25	96.89	2.81	0.30
	50	97.87	1.95	0.18	97.03	2.75	0.22
2	10	97.83	1.88	0.29	97.15	2.50	0.35
	30	97.61	2.08	0.31	96.85	2.77	0.38
	50	97.47	2.26	0.27	96.57	3.11	0.32

water and oxygen gas due to thermal effects. This excessive decomposition would waste the reductant and generate significant gas pressure, compromising both efficiency and safety. Van Benschoten et al. [40] and Freitas et al. [41] report high Mn recovery rates (>99,5%) through similar oxidative precipitation methods. Consequently, the high purity achieved within the tested parameters confirms the stability and operational effectiveness of this recovery process. Residual $ZnSO_4$ and NH_4Cl impurities persist in the final product due to the porous morphology of MnO_2 that facilitates the diffusion and subsequent entrapment of Zn^{2+} and Cl^- ions within the internal pore structure of the manganese dioxide precipitate [42, 43].

3.2 Effect of reductant addition and time

Manganese leaching via microwave irradiation reduces Mn^{4+} to soluble Mn^{2+} in H_2SO_4 to produce $MnSO_4$. While the process occurs independently, reductants like H_2O_2 significantly optimize the efficiency, achieving recovery rates as high as 99.04% in manganese ore leaching [25, 27, 28]. Microwave energy accelerates this redox reaction by enhancing molecular collisions and ionic mobility, which destabilizes Mn–O bonds in the MnO_6 octahedral framework. Compared to conventional heating, microwave-assisted methods offer a 20% increase in efficiency [25]. The resulting Mn^{2+} is subsequently converted into high-purity MnO_2 through $KMnO_4$ precipitation. Reaction mechanism in leaching process is shown in Eqs. (6) and (7) without H_2O_2 as reductant, in Eqs. (8) and (9) with H_2O_2 reductant [44, 45].

$$2MnO_{2(s)} + 2H_2SO_{4(aq)} \rightarrow 2MnSO_{4(aq)} + 2H_2O_{(l)} + O_{2(g)} \quad (6)$$

$$Zn_{(s)} + 2H_2SO_{4(aq)} \rightarrow ZnSO_{4(aq)} + SO_{2(g)} + 2H_2O_{(l)} \quad (7)$$

$$MnO_{2(s)} + H_2O_{2(aq)} + H_2SO_{4(aq)} \rightarrow MnSO_{4(aq)} + 2H_2O_{(l)} + O_{2(g)} \quad (8)$$

$$2Zn_{(s)} + 2H_2O_{2(aq)} + 2H_2SO_{4(aq)} \rightarrow 2ZnSO_{4(aq)} + 4H_2O_{(l)} \quad (9)$$

The influence of H_2O_2 concentration on MnO_2 recovery, as illustrated in Fig. 3, demonstrates that the

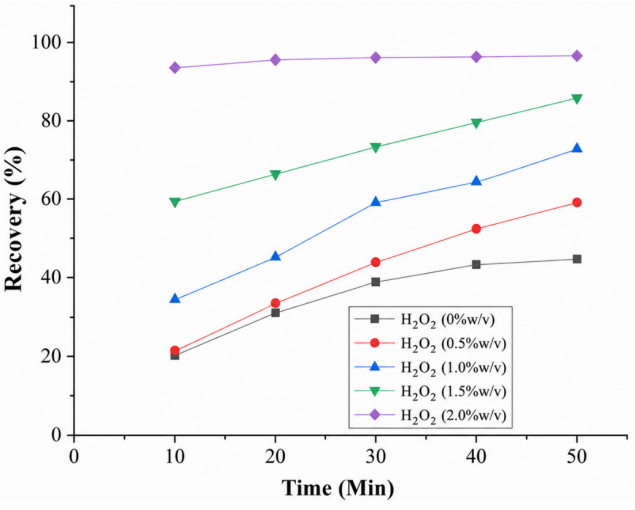

Fig. 3 The effect of reductant concentration on recovery efficiency

recovery efficiency is highly dependent on the presence of a reducing agent to convert inert Mn^{4+} into soluble Mn^{2+} [46]. Without H_2O_2, the recovery remained below 40%, whereas the addition of 0.5–1% w/v H_2O_2 significantly enhanced the recovery to approximately 88% by providing active peroxide species that lower the activation energy of the reduction process [11]. The optimum recovery of approximately 96% was achieved at 2% w/v H_2O_2 within 20–50 min, representing a stoichiometric balance between the reductant and the metal oxide. However, increasing the concentration beyond 2% w/v resulted in decreased efficiency due to the rapid thermal decomposition of H_2O_2 into O_2 under microwave irradiation and the potential back-oxidation of Mn^{2+} ions [47]. The kinetic profiles indicate a rapid initial leaching phase in the first 10 min followed by stabilization, confirming that the combination of microwave activation and 2% w/v H_2O_2 provides the most effective conditions for maximizing MnO_2 recovery from spent dry cell batteries [27].

3.3 MnO_2 precipitation

To accurately determine the true recovery of manganese from the spent dry cells, a rigorous mass balance was applied during the precipitation stage. Oxidative precipitation using $KMnO_4$ was selected because it has high selectivity and provides a high recovery yield up to 99.9% [41]. The reaction mechanism in precipitation process is shown in Eqs. (10) and (11) [44, 45].

$$3Mn^{2+} + 2MnO_4^- + 2H_2O \rightarrow 5MnO_2 + 4H^+ \quad (10)$$

$$3MnSO_{4(aq)} + 2KMnO_{4(aq)} + 2H_2O_{(l)} \rightarrow 5MnO_{2(s)} + 2H_2SO_{4(aq)} + K_2SO_{4(aq)} \quad (11)$$

Based on Eqs. (8) and (11), the amount of leached MnO_2 from dry cell and MnO_2 recovery can be calculated using Eqs. (12)–(14).

$$m_{MnO_2,final} = \%_{MnO_2} \times m_{precipitate} \quad (12)$$

$$m_{MnO_2,leached} = \frac{3}{5} \times m_{MnO_2,final} \quad (13)$$

$$Recovery = \frac{m_{MnO_2,leached}}{m_{MnO_2,dry\ cell}} \times 100\% \quad (14)$$

The $m_{precipitate}$ is the mass of the precipitate (g), $m_{MnO_2,leached}$ is the mass of MnO_2 leached from the dry cell (g), $m_{MnO_2,final}$ is the mass of MnO_2 precipitated (g), $m_{MnO_2,dry\ cell}$ is the mass of MnO_2 in the dry cell (g) and $\%_{MnO_2}$ is the purity of MnO_2 in the precipitate (%). Results of the calculations from Eqs. (12)–(14) are shown in Fig. 3.

The final MnO_2 precipitate originates from two distinct sources: the dissolved Mn^{2+} extracted from the dry cell waste, and the reduction of the $KMnO_4$ reagent itself. Based on the stoichiometric ratio, exactly 2 mol $KMnO_4$ are consumed to precipitate 3 mol of dissolved Mn^{2+}, resulting in 5 mol of MnO_2. From the precise titration volume of 0.25 M $KMnO_4$ required to completely precipitate the dissolved Mn, the mass of manganese originating from the permanganate was explicitly calculated (Table 5). To eliminate any positive bias, this reagent-derived manganese mass was subtracted from the total mass of the final precipitate. Consequently, the reported recovery percentages strictly reflect the true mass of manganese successfully extracted and recovered solely from the battery waste matrix.

Otherwise, there are some processes for MnO_2 precipitation. Table 6 shows that the permanganate oxidative precipitation provides the highest recovery (99.5–99.9%) but involves strong oxidants and higher costs [40, 41]. Electrolysis offers a cleaner process (93%) but requires high energy and expensive electrodes [48].

Table 5 Amount of $KMnO_4$ precipitator and MnO_2 precipitate

Factor H_2O_2 (%w/v)	Time (min)	Volume of 0.25 M $KMnO_4$ (mL)	*m* precipitate (g)
0	10	43.0	2.25
	20	65.3	3.48
	30	80.6	4.32
	40	89.1	4.79
	50	92.6	4.98
0.5	10	46.1	2.42
	20	71.1	3.80
	30	91.5	4.92
	40	108.0	5.83
	50	122.0	6.60
1	10	72.4	3.87
	20	94.2	5.07
	30	122.0	6.60
	40	134.2	7.27
	50	149.4	8.11
1.5	10	121.1	6.55
	20	134.3	7.28
	30	148.7	8.07
	40	160.0	8.69
	50	173.6	9.44
2	10	190.8	10.39
	20	193.9	10.56
	30	196.6	10.71
	40	195.9	10.67
	50	198.1	10.79

Table 6 MnO_2 precipitation process

Process	Material	Recovery (%)	Reference
Permanganate oxidative precipitation	$KMnO_4$	99.5–99.9	[40, 41]
Electrolysis	Ti/IrO_2	93	[48]
Oxalate precipitation (calcination precursor)	$H_2C_2O_4$ (Oxalic acid)	96	[49]
Carbonate precipitation	Na_2CO_3	93.4	[50]
	$(NH_4)_2CO_3$	90.8	[51]
Persulfate oxidative precipitation	$(NH_4)_2S_2O_8$	95.5	[52]

Oxalate precipitation (96%) works under milder conditions but needs additional calcination and handling of organic reagents [49]. Carbonate methods (90.8–93.4%) are simpler and cheaper, though with lower recovery and needs additional calcination [50, 51]. Persulfate oxidation (95.5%) gives good efficiency but may increase cost and introduce sulfate residues [52].

3.4 Optimization

A total of 10 runs were calculated following the face centered central composite design protocol as shown in Table 7. The hydrometallurgical process to recover MnO_2 was executed according to each designated set point. Table 7 also presents the experimental and predicted glucose response values for comparison.

The linear model was identified as the most suitable fit due to its superior value on adjusted R^2 (0.8908) and predicted R^2 (0.8071), coupled with a lower sequential p-value (0.0002) and a high lack of fit p-value (0.1952). Consequently, this model was selected for the ANOVA modeling presented in Table 8. A smaller p-value ($p < 0.05$) indicates a higher probability of significant variable validity. While R^2 determines the relationship between response and independent variables, the adjusted R^2 reflects the actual variability within the equation regarding data distribution; therefore, both values should ideally approach 1.0 [53].

Table 7 RSM design experimental and predicted value

Run	Factor A: H_2O_2 (%w/v)	Factor B: Time (min)	Response Y: Recovery (%)	
			Experimental	Predicted
1	1	30	59.15	61.27
2	0	30	38.95	30.77
3	2	30	96.32	91.76
4	1	30	55.57	61.27
5	1	50	72.70	72.19
6	0	50	44.64	41.70
7	1	10	34.57	50.34
8	0	10	20.26	19.85
9	2	50	96.76	102.69
10	2	10	93.74	80.84

Based on Table 8, the experimental data were fitted to a linear polynomial model represented by Eq. (15).

$$Y = 14.3851 + 30.49362 \times A + 0.546262 \times B \quad (15)$$

The Y denotes the recovery rate (%) and variables A (reductant dosage) and B (time) serve as independent factors. ANOVA results confirm the model's high statistical significance, evidenced by an F-value of 37.72 and a mere 0.02% probability of noise interference. While both factors are significant ($p < 0.05$), factor A exhibits a higher level of significance than B. The model's adequacy is further validated by a non-significant lack of fit (F = 14.98, p = 0.1952), an R^2 of 0.9151, and a close agreement between adjusted and predicted R^2 (difference < 0.2). Finally, an adequate precision of 16.5559 confirms a robust signal-to-noise ratio, exceeding the required threshold of 4 [54].

The strong correlation between the predicted and actual values, as illustrated in Fig. 4, underscores the reliability and accuracy of the model in forecasting manganese recovery during the leaching process. This visual representation confirms that the model consistently captures the relationship between simulation results and experimental data across various time frames and reductant types. In the plot of predicted versus experimental results, the close proximity of data points to the linear regression line indicates an excellent model fit. Consequently, the alignment of these data points suggests that the mathematical model effectively accounts for the impact of reaction time and reductant dosage on manganese recovery within the hydrometallurgical process [55].

Fig. 5 presents the contour and three-dimensional response surface plots, illustrating the interactive effects of H_2O_2 dosage (A) and reaction time (B) on manganese recovery during the microwave-assisted hydrometallurgical leaching. The color spectrum within these plots serves as a qualitative measure of recovery efficiency: warmer tones transitioning toward red denote higher response values, while cooler shades, such as blue and green, signify reduced yields [56]. These color variations highlight the significant influence of H_2O_2 as a reductant on the dissolution of manganese dioxide, with the maximum recovery localized in the red regions of the plots. Consequently,

Table 8 ANOVA results for the predictive modeling of recovery in hydrometallurgical processing

Source	Sum of squares	*df*	Mean square	*F*-value	*p*-value	
Model	6295.33	2	3147.66	37.72	0.0002	Significant
A: H_2O_2	5579.17	1	5579.17	66.86	<0.0001	
B: Time	716.16	1	716.16	8.58	0.0220	
Residual	584.15	7	83.45			
Lack of fit	577.73	6	96.29	14.98	0.1952	not significant
Pure error	6.43	1	6.43			
Corrected total	6879.48	9				
Fit statistics						
Std. Dev.	9.14		R^2	0.9151		
Mean	61.27		Adjusted R^2	0.8908		
C.V. %	14.91		Predicted R^2	0.8071		
			Adequate precision	16.5559		

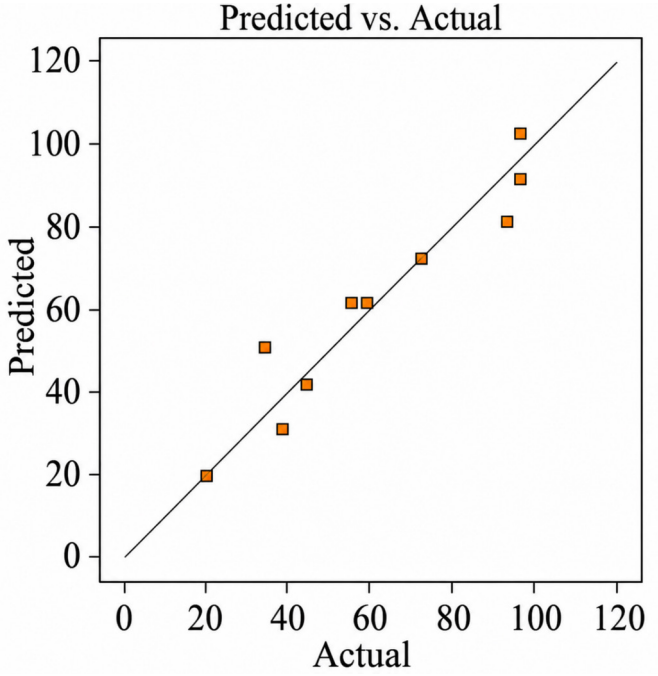

Fig. 4 Predicted vs. actual plot for the recovery of MnO_2

it can be observed that a synergistic increase in both the H_2O_2 concentration and reaction time leads to a substantial enhancement in the manganese recovery.

Utilizing the derived regression model based on Eq. (15), the predicted optimum yield was determined to be 96.8% under an H_2O_2 dosage 2% w/v and a duration 39.15 min (Table 9). Desirability was employed as a metric to evaluate the alignment of the optimal solution with the targeted responses, where a value of 1 signifies a perfect scenario [57]. A desirability score exceeding 0.8 is generally required for robust process optimization [54]. These findings demonstrate that both H_2O_2 concentration and reaction time exert significant, interrelated influences on the manganese recovery rate, with the peak of the response surface plot identifying the ideal conditions for maximizing process efficiency.

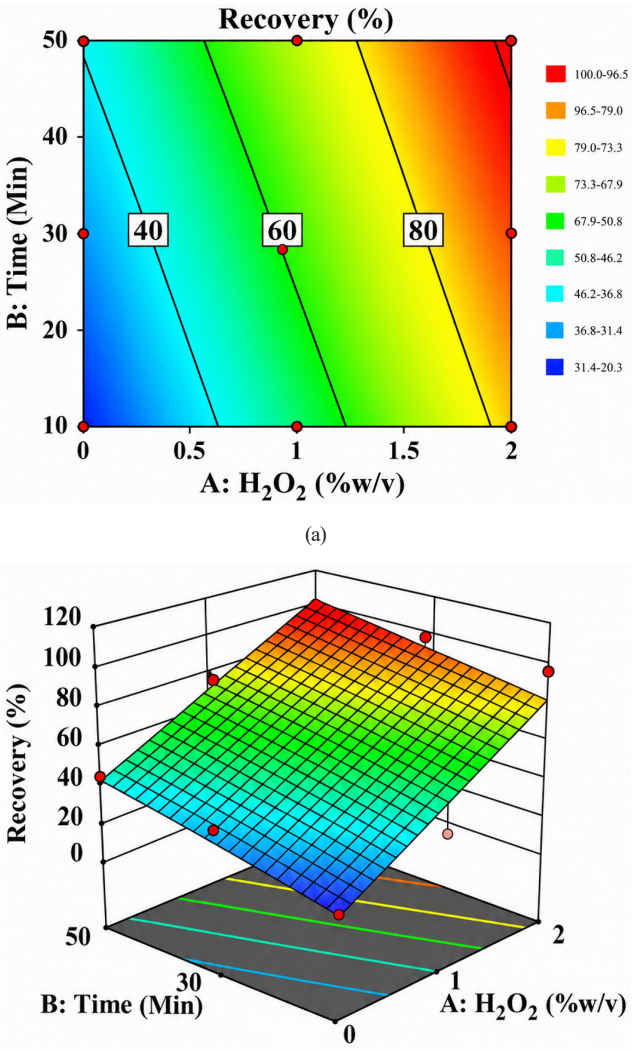

(a)

(b)

Fig. 5 (a) Contour plot and (b) 3D response surface plot illustrating the interaction between factor *A* and *B* on manganese recovery

Table 9 Numerical optimation results

Name	Goal	Lower limit	Upper limit	Lower weight	Upper weight
A: H_2O_2	is in range	0	2	1	1
B: Time	Minimize	10	50	1	1
Recovery	Maximize	90	96.7608	1	1
A: H_2O_2 (%w/v)	*B*: Time (min)	Recovery (%)	Composite desirability		
2	39.154	96.761	0.805		

4 Conclusion

While metallic impurities such as zinc are readily soluble in dilute acids, extracting manganese from spent dry cell batteries is highly challenging due to the chemical stability and insolubility of MnO_2. This study demonstrates that overcoming this barrier necessitates a synergistic approach using microwave-assisted heating and H_2O_2 as a reducing agent. The reductant is strictly required to convert the inert Mn^{4+} into soluble Mn^{2+}, while the microwave energy drastically accelerates the reaction kinetics. The permanganate oxidative precipitation is the simplest process and most efficient method with the highest recovery, but it comes with higher cost and handling complexity. Other methods such as electrolysis, oxalate, carbonate and persulfate precipitation offer more practical or economical alternatives, though generally with slightly lower recovery. Optimization via RSM and CCD identified the ideal conditions as 2% w/v H_2O_2 and a leaching time of 39.15 min, resulting in a verified MnO_2 recovery of 96.8%. The recovered product achieved a high MnO_2 purity of 96–97%, surpassing the standard commercial electrolytic manganese dioxide (EMD) threshold > 92%.

In contribution to the state of the art, this study proves that the integration of microwave irradiation and chemical reduction accelerates the processing time to under 40 min, offering a significant advantage over conventional methods. This integrated approach not only provides a highly time- and energy-efficient pathway for valorizing hazardous spent dry cell batteries but also offers a viable technical framework for scaling up secondary manganese resource recovery. Consequently, future research should explore variables, such as acid concentration range, solid-to-liquid ratios and microwave power levels, to further refine the purity and gain a comprehensive understanding of the process kinetics.

Acknowledgement

Authors thank our colleagues from Universitas Pembangunan Nasional "Veteran" Jawa Timur who provided insight and expertise that greatly assisted the research.

References

[1] Hasim, A., Hermawan, A., Prastyo, A. "Penyisihan Kadar Besi (Fe) dan Mangan (Mn) dalam Air Sumur dengan Media Pasir Terlapis Mangan Dioksida" (Iron and Manganese Deposits in Well Water with an Encrusted Sandpaper), Jurnal Bhuwana, 2(1), pp. 45–56, 2022. (in Indonesian) https://doi.org/10.25105/bhuwana.v2i1.14462

[2] Zhang, Y., Fan, X., Hu, W., Luo, Z., Yang, Z., Li, G., Li, Y. "Microstructure and magnetic properties of MnO_2 coated iron soft magnetic composites prepared by ball milling", Journal of Magnetism and Magnetic Materials, 514, 167295, 2020. https://doi.org/10.1016/j.jmmm.2020.167295

[3] Hendratna, A. "The Application of MnO_2 and $KMnO_4$ for Persistent Organic Compounds and COD Removals in Wastewater Treatment Process, Master Thesis, Royal Institute of Technology (KTH), 2011.

[4] Badan Pusat Statistik "Data Impor Manganese Dioxide" (Manganese Dioxide Import Data), [online] Available at: https://www.bps.go.id/id (Data retrieved through search using HS Code: 28201000) [Accessed: 06 January 2025] (in Indonesian)

[5] Rahman, M. A., Hashem, M. A., Rana, M. S., Islam, M. R. "Manganese in potable water of nine districts, Bangladesh: human health risk", Environmental Science and Pollution Research, 28(33), pp. 45663–45675, 2021. https://doi.org/10.1007/s11356-021-14016-z

[6] Perry, R. H., Green, D. W., Maloney, J. O. "Perry's Chemical Engineers' Handbook", McGraw-Hill, 1997. ISBN 0-07-049841-5

[7] Dawadi, S., Gupta, A., Khatri, M., Budhathoki, B., Lamichhane, G., Parajuli, N. "Manganese dioxide nanoparticles: synthesis, application and challenges", Bulletin of Materials Science, 43(1), 277, 2020. https://doi.org/10.1007/s12034-020-02247-8

[8] Carbone, R. "Energy Storage in the Emerging Era of Smart Grids", IntechOpen, 2011. ISBN 978-953-307-269-2 https://doi.org/10.5772/737

[9] Ministry of Health Republic of Indonesia "Peraturan Menteri Kesehatan Republic Indonesia Nomor 2 Tahun 2023 tentang Peraturan Pelaksanaan Peraturan Pemerintah Nomor 66 Tahun 2014 tentang Kesehatan Lingkungan" (Regulation of the Minister of Health of the Republic of Indonesia Number 2 of 2023 concerning Implementing Regulations of Government Regulation Number 66 of 2014 concerning Environmental Health), Jakarta, Indonesia, 2023. (in Indonesian)

[10] Matveeva, V. A., Alekseenko, A. V., Karthe, D., Puzanov, A. V. "Manganese Pollution in Mining-Influenced Rivers and Lakes: Current State and Forecast under Climate Change in the Russian Arctic", Water, 14(7), 1091, 2022. https://doi.org/10.3390/w14071091

[11] Zhu, J., Wang, Y., Huang, Y., Bhushan Gopaluni, R., Cao, Y., …, Ehrenberg, H. "Data-driven capacity estimation of commercial lithium-ion batteries from voltage relaxation", Nature Communications, 13(1), 2261, 2022. https://doi.org/10.1038/s41467-022-29837-w

[12] George, A. T., Ganesan, R., Thangeeswari, T. "Redox Deposition of Manganese Oxide Nanoparticles on Graphite Electrode by Immersion Technique for Electrochemical Super Capacitors", Indian Journal of Science and Technology, 9(1), pp. 1–7, 2016. https://doi.org/10.17485/ijst/2016/v9i1/85782

[13] Igharo, K. O. "Construction of a Primary Dry Cell Battery from Cassava Juice Extracts (The Cassava Battery Cell)", Journal of Educational and Social Research, 2(8), pp. 18–23, 2012. https://doi.org/10.5901/jesr.2012.v2n8p18

[14] Sawyer, D. T. "Electrochemistry", In: Meyers, R. A. (ed.) Encyclopedia of Physical Science and Technology, Academic Press, 2003, pp. 161–197. ISBN 978-0-12-227410-7 https://doi.org/10.1016/B0-12-227410-5/00206-4

[15] Sonule, B. B., Kulkarni, A. N., Kakde, N. K., Madrewar, K. T. "Comparative Analysis of Pyrometallurgy, Hydrometallurgy and Bio-Hydro-Metallurgy for Extraction of Metals from E-Waste", International Journal of Research Publication and Reviews, 4(10), pp. 1970–1977, 2023.

[16] Mirahati, R. Z. "Studi Pustaka Potensi Ekstraksi Logam dari Limbah Elektronik dengan Bioleaching" (Literature Study on the Potential of Metal Extraction from Electronic Waste by Bioleaching), Jurnal Teknologi Pertambangan, 5(2), pp. 153–159, 2019. (in Indonesian)

[17] Joulié, M., Laucournet, R., Billy, E. "Hydrometallurgical process for the recovery of high value metals from spent lithium nickel cobalt aluminum oxide based lithium-ion batteries", Journal of Power Sources, 247, pp. 551–555, 2014. https://doi.org/10.1016/j.jpowsour.2013.08.128

[18] Jimenez de Aberasturi, D., Pinedo, R., Ruiz de Larramendi, I., Ruiz de Larramendi, J. I., Rojo, T. "Recovery by hydrometallurgical extraction of the platinum-group metals from car catalytic converters", Minerals Engineering, 24(6), pp. 505–513, 2011. https://doi.org/10.1016/j.mineng.2010.12.009

[19] Quijada-Maldonado, E., Olea, F., Sepúlveda, R., Cabezas, R., Merlet, G., Romero, J. "Possibilities and challenges for ionic liquids in hydrometallurgy", Separation and Purification Technology, 251, 117289, 2020. https://doi.org/10.1016/j.seppur.2020.117289

[20] Zheng, X., Zhu, Z., Lin, X., Zhang, Y., He, Y., Cao, H., Sun, Z. "A Mini-Review on Metal Recycling from Spent Lithium Ion Batteries", Engineering, 4(3), pp. 361–370, 2018. https://doi.org/10.1016/j.eng.2018.05.018

[21] Bertuol, D. A., Tanabe, E. H., Meili, L., Veit, H. M. "Hydrometallurgical Processing", In: Veit, H. M., Moura Bernardes, A. (eds.) Electronics Waste, Springer, 2015, pp. 61–71. ISBN 978-3-319-15713-9 https://doi.org/10.1007/978-3-319-15714-6_6

[22] You, Z., Li, G., Zhang, Y., Peng, Z., Jiang, T. "Extraction of manganese from iron rich MnO_2 ores via selective sulfation roasting with SO_2 followed by water leaching", Hydrometallurgy, 156, pp. 225–231, 2015. https://doi.org/10.1016/j.hydromet.2015.05.017

[23] Behera, S. S., Panda, S. K., Mandal, D., Parhi, P. K. "Ultrasound and Microwave assisted leaching of neodymium from waste magnet using organic solvent", Hydrometallurgy, 185, pp. 61–70, 2019. https://doi.org/10.1016/j.hydromet.2019.02.003

[24] Desai, M., Parikh, J., Parikh, P. A. "Extraction of Natural Products Using Microwaves as a Heat Source", Separation & Purification Reviews, 39(1–2), pp. 1–32, 2010. https://doi.org/10.1080/15422111003662320

[25] Lin, S., Gao, L., Yang, Y., Chen, J., Guo, S., Omran, M., Chen, G. "Efficiency and sustainable leaching process of manganese from pyrolusite-pyrite mixture in sulfuric acid systems enhanced by microwave heating", Hydrometallurgy, 198, 105519, 2020. https://doi.org/10.1016/j.hydromet.2020.105519

[26] Chang, J., Srinivasakannan, C., Sun, X., Jia, F. "Optimization of microwave-assisted manganese leaching from electrolyte manganese residue", Green Processing and Synthesis, 9(1), pp. 2–12, 2020. https://doi.org/10.1515/gps-2020-0001

[27] Tian, X., Wen, X., Yang, C., Liang, Y., Pi, Z., Wang, Y. "Reductive leaching of manganese from low-grade manganese dioxide ores using corncob as reductant in sulfuric acid solution", Hydrometallurgy, 100(3–4), pp. 157–160, 2010. https://doi.org/10.1016/j.hydromet.2009.11.008

[28] Nayl, A. A., Ismail, I. M., Aly, H. F. "Recovery of pure $MnSO_4 \cdot H_2O$ by reductive leaching of manganese from pyrolusite ore by sulfuric acid and hydrogen peroxide", International Journal of Mineral Processing, 100(3–4), pp. 116–123, 2011. https://doi.org/10.1016/j.minpro.2011.05.003

[29] Anderson, M. J., Whitcomb, P. J. "RSM Simplified: Optimizing Processes Using Response Surface Methods for Design of Experiments", Productivity Press, 2016. ISBN 9781498745987

[30] Ait-Amir, B., Pougnet, P., El Hami, A. "6 - Meta-Model Development", In: El Hami, A., Pougnet, P. (eds.) Embedded Mechatronic Systems 2: Analysis of Failures, Modeling, Simulation and Optimization, Elsevier, 2015, pp. 151–179. ISBN 978-1-78548-014-0 https://doi.org/10.1016/B978-1-78548-014-0.50006-2

[31] Pereira, L. M. S., Milan, T. M., Tapia-Blácido, D. R. "Using Response Surface Methodology (RSM) to optimize 2G bioethanol production: A review", Biomass and Bioenergy, 151, 106166, 2021. https://doi.org/10.1016/j.biombioe.2021.106166

[32] Shishir, M. R. I., Chen, W. "Trends of spray drying: A critical review on drying of fruit and vegetable juices", Trends in Food Science & Technology, 65, pp. 49–67, 2017. https://doi.org/10.1016/j.tifs.2017.05.006

[33] Veza, I., Spraggon, M., Fattah, I. M. R., Idris, M. "Response surface methodology (RSM) for optimizing engine performance and emissions fueled with biofuel: Review of RSM for sustainability energy transition", Results in Engineering, 18, 101213, 2023. https://doi.org/10.1016/j.rineng.2023.101213

[34] Fattahi, A., Rashchi, F., Abkhoshk, E. "Reductive leaching of zinc, cobalt and manganese from zinc plant residue", Hydrometallurgy, 161, pp. 185–192, 2016. https://doi.org/10.1016/j.hydromet.2016.02.003

[35] Khosravi, R., Fatahi, R., Siavoshi, H., Molaei, F. "Recovery of Manganese from Zinc Smelter Slag", American Journal of Engineering and Applied Sciences, 13(4), pp. 748–758, 2020. https://doi.org/10.3844/ajeassp.2020.748.758

[36] Karacahan, M. K. "Optimization and Kinetic Study of Manganese Leaching from Pyrolusite Ore in Hydrochloric Acid Solutions with Oxalic Acid", Journal of Sustainable Metallurgy, 10(3), pp. 1717–1732, 2024. https://doi.org/10.1007/s40831-024-00869-4

[37] ASTM "ASTM E465-24 Standard Test Methods for Determination of Manganese (IV) in Manganese Ores by Redox Titrimetry", ASTM International, West Conshohocken, PA, USA, 2024. https://doi.org/10.1520/E0465-24

[38] StatEase "Design Expert, (Version 13.00)", [computer program] Available at: https://www.statease.com/software/design-expert/ [Accessed: 17 February 2026]

[39] Peng, C., Chang, C., Wang, Z., Wilson, B. P., Liu, F., Lundström, M. "Recovery of High-Purity MnO_2 from the Acid Leaching Solution of Spent Li-Ion Batteries", JOM, 72(2), pp. 790–799, 2020. https://doi.org/10.1007/s11837-019-03785-1

[40] Van Benschoten, J. E., Lin, W., Knocke, W. R. "Kinetic modeling of manganese(II) oxidation by chlorine dioxide and potassium permanganate", Environmental Science & Technology, 26(7), pp. 1327–1333, 1992. https://doi.org/10.1021/es00031a008

[41] Freitas, R. M., Perilli, T. A. G., Ladeira, A. C. Q. "Oxidative precipitation of manganese from acid mine drainage by potassium permanganate", Journal of Chemistry, 2013(1), 287257, 2013. https://doi.org/10.1155/2013/287257

[42] Osipov, A. R., Kiselev, A. D., Kraidenko, R. I., Borisov, V. A. "A study on the interaction of manganese dioxide with ammonium chloride", AIP Conference Proceedings, 2141(1), 020023, 2019. https://doi.org/10.1063/1.5122042

[43] Zheng, Y., Chen, D., Zhao, Y., Bao, H., Sun, Y. "Elucidating the diffusion and interaction mechanisms of Zn^{2+} and H^+ in MnO_2 for aqueous zinc-ion batteries: A DFT study", Journal of Power Sources, 625, 235658, 2025. https://doi.org/10.1016/j.jpowsour.2024.235658

[44] Vogel, A. I. "Vogel's Textbook of Macro and Semimicro Qualitative Inorganic Analysis", Longman, 1979. ISBN 978-0582443679

[45] Jeffery, G. H., Bassett, J., Mendham, J., Denney, R. C. "Vogel's textbook of quantitative chemical analysis", Longman, 1989. ISBN 0-582-44693-7

[46] Baba, A. A., Ibrahim, L., Adekola, F. A., Bale, R. B., Ghosh, M. K., Sheik, A. R., Pradhan, S. R., Ayanda, O. S., Folorunsho, I. O. "Hydrometallurgical Processing of Manganese Ores: A Review", 2(3), pp. 230–247, 2014. https://doi.org/10.4236/jmmce.2014.23028

[47] Kauppinen, T., Vielma, T., Salminen, J., Lassi, U. "Selective Recovery of Manganese from Anode Sludge Residue by Reductive Leaching", ChemEngineering, 4(2), 40, 2020. https://doi.org/10.3390/chemengineering4020040

[48] Ntunka, M., Loveday, B. "Sustainable production of electrolytic manganese dioxide (EMD): A conceptual flowsheet", Cleaner Chemical Engineering, 11, 100145, 2025. https://doi.org/10.1016/j.clce.2024.100145

[49] Gudim da Silva, R., Nunes da Silva, C., Afonso, J. C. "Recovery of Manganese and Zinc from Spent Zn-C and Alkaline Batteries in Acidic Medium", Química Nova, 33(9), pp. 1957–1961, 2010. https://doi.org/10.1590/S0100-40422010000900024

[50] Andak, B., Özduğan, E., Türdü, S., Bulutcu, A. N. "Recovery of zinc and manganese from spent zinc-carbon and alkaline battery mixtures via selective leaching and crystallization processes", Journal of Environmental Chemical Engineering, 7(5), 103372, 2019. https://doi.org/10.1016/j.jece.2019.103372

[51] Nogueira, C. A., Margarido, F. "Selective process of zinc extraction from spent Zn–MnO_2 batteries by ammonium chloride leaching", Hydrometallurgy, 157, pp. 13–21, 2015. https://doi.org/10.1016/j.hydromet.2015.07.004

[52] Yu, W., Li, X., Xu, W., Guan, Q., Zhou, F., Zhang, J., Wang, L., Wang, Y., Tang, H. "Advances in Electrolytic Manganese Residue: Harmless Treatment and Comprehensive Utilization", 12(7), 180, 2025. https://doi.org/10.3390/separations12070180

[53] Chen, H.-Y., Chen, C. "A Study of the Response Surface Methodology Model with Regression Analysis in Three Fields of Engineering", Applied System Innovation, 8(4), 99, 2025. https://doi.org/10.3390/asi8040099

[54] Fazeli Burestan, N., Afkari Sayyah, A. H., Taghinezhad, E. "Mathematical modeling for the prediction of some quality parameters of white rice based on the strength properties of samples using response surface methodology (RSM)", Food Science & Nutrition, 8(8), pp. 4134–4144, 2020. https://doi.org/10.1002/fsn3.1703

[55] Sreekumar, S., Chakrabarti, S., Hewitt, N., Mondol, J. D., Shah, N. "Performance Prediction and Optimization of Nanofluid-Based PV/T Using Numerical Simulation and Response Surface Methodology", Nanomaterials, 14(9), 774, 2024. https://doi.org/10.3390/nano14090774

[56] Tassano, E., Faber, K., Hall, M., "Biocatalytic Parallel Interconnected Dynamic Asymmetric Disproportionation of α-Substituted Aldehydes: Atom-Efficient Access to Enantiopure (*S*)-Profens and Profenols", Advanced Synthesis & Catalysis, 360(14), pp. 2742–2751, 2018. https://doi.org/10.1002/adsc.201800541

[57] Redhwan, A. A. M., Azmi, W. H., Sharif, M. Z., Zawawi, N. N. M., Zainal Ariffin, S. "Utilization of Response Surface Method (RSM) in Optimizing Automotive Air Conditioning (AAC) Performance Exerting Al_2O_3/PAG Nanolubricant", Journal of Physics: Conference Series, 1532(1), 012003, 2020. https://doi.org/10.1088/1742-6596/1532/1/012003